

Analysis of Stabilization and Extrapolation Methods for Determining Energies and Lifetimes of Metastable Electronic States

Published as part of *The Journal of Physical Chemistry virtual special issue "125 Years of The Journal of Physical Chemistry"*.

Jack Simons*



Cite This: *J. Phys. Chem. A* 2021, 125, 7735–7749



Read Online

ACCESS |



Metrics & More



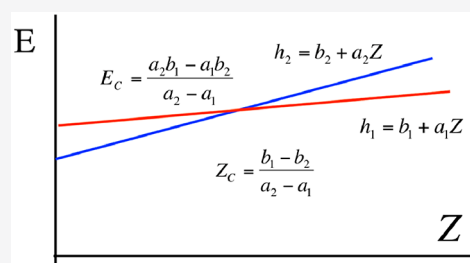
Article Recommendations



Supporting Information

ABSTRACT: Two methods that make use of standard electronic structure tools, the stabilization and extrapolation methods, are discussed with an eye toward pointing out their relative strengths and weaknesses and for improving their applications. In the former, whether to utilize energy data from only one or from both branches of an avoided crossing between the quasi-bound and pseudo-continuum states is one issue that is focused on. Another is the decision of where along the stabilization plot's branches (i.e., far from or close to the avoided crossing) to create data points for optimal performance given a reasonable (10^{-5} – 10^{-7} eV) precision in the electronic energy. A third issue is how many parameters to use in fitting energy data to the (one or two) branches of the stabilization plot. In

extrapolation methods, one uses energy data computed when the metastable state's energy has been rendered stable by the application of an external potential, which thus produces a one-branch function. The main issues in implementing this method are the functional form for how the energy E depends on the strength of the external potential especially as the energy evolves from the bound-state region toward the unbound region and how to choose data points so that energy values of a reasonable precision are capable of determining the parameters in the formula that produces the metastable state's energy E and half-width $\Gamma/2$ (inversely related to the state's lifetime). In addition to explaining, critiquing, and comparing these two methods, several suggestions are offered for their further testing and improvements.



1. INTRODUCTION

It is my hope that the analysis and insights offered in this paper will allow a wider range of scientists to make use of stabilization and extrapolation methods for characterizing anions that are electronically quasi-bound. I think this is important because the currently available quantum chemistry software now includes pathways for examining such situations, which means that the number of workers doing so is bound to grow. In addition to attracting new workers to this field, I hope that current practitioners and developers of these tools will gain knowledge that will help them sharpen and focus the methods they have pioneered.

Calculating the energy and lifetime of an electronically metastable anion is a difficult task^{1–3} because the electronic state is imbedded within a continuum of other states belonging to the neutral molecule plus a free electron. This means that the state of interest is not the lowest-energy state of its symmetry, so the wide range of variational methods used to compute ground and excited bound states cannot straightforwardly be of use. However, much progress has been and is being made on developing new computational tools to address the problem although many of them require substantial modifications to the electronic structure computer programs, and such methods are

not being discussed here. There are two approaches that have been especially useful in characterizing metastable species that make use of conventional electronic structure codes with little modification. This paper attempts to describe two of them: so-called stabilization methods and extrapolation methods. A primary goal is to clarify some of the pitfalls, strengths, and weaknesses of these tools aiming primarily at an audience of mainstream electronic structure theory users who are not yet informed about them. Along those lines, I offer several suggestions for further testing and improvements.

In the most widely used conventional stabilization methods^{4–8} (SMs), one tries to use an orbital basis set that is capable of describing the core and valence-range electronic structure of the neutral molecule, of the anion formed by attaching an electron, as well as continuum states corresponding to the neutral molecule plus a free electron having an energy close to

Received: May 1, 2021

Revised: August 11, 2021

Published: August 24, 2021



that of the metastable anion. One then computes the energies of several states⁹ in a range within which a metastable state is expected. This process of computing several states' energies is then repeated as the radial extents of the more diffuse basis orbitals are scaled. The possible existence of a metastable state is signaled by the occurrence of one state's energy remaining relatively stable over a significant set of scaled basis sets. The plateauing or stabilization of this energy is the key feature of this approach. How the lifetime of the metastable state is extracted will be explained in section 2.

In extrapolation methods^{10–17} (EMs) one adds to the Hamiltonian of the electron-attached species a potential V_{att} that serves to differentially stabilize the energy of electrons in the core and valence regions relative to the energy of electrons that are more distant. For example, in studying¹⁸ the metastable SO_4^{2-} , the charge of the sulfur nucleus can be increased from 16 to $16 + x$ to achieve this differential stabilization. Clearly, at $x = 1.0$, the system would be a geometrically distorted (because ClO_4^- does not have the same bond lengths as sulfate) ClO_4^- anion, which is stable, not metastable. By performing calculations in which the added stabilizing potential's strength (Z) is increased to varying degrees, one eventually reaches a point at which the electron-attached species become electronically stable. From this point on, one can use conventional electronic structure tools to compute the electronic energy of this artificially stabilized species. If one has a theoretical framework within which to extrapolate the electronic energy from values of Z where the species is bound into regions of Z where it is metastable and onward to $Z = 0$, such a tool can be used to predict the energy and lifetime of the metastable species. The key to such EMs is to use the correct analytical structures for expressing how the energy E depends on the strength parameter Z , especially in the region where E moves from electronically bound to unbound. These analytical formulas will be explained in section 3.

2. STABILIZATION METHODS

2A. Stabilization Plots. Perhaps the most common variant of the SM involves scaling the atomic orbital exponents of several of the most diffuse basis functions thereby varying the radial extent of the basis set. One first computes the energies of several electronic states of the electron-attached species and subtracts each such energy from the energy of the parent species in the absence of the excess electron. The latter energy will also vary as one scales the basis orbitals, albeit less so than for the energies of the electron-attached states. One then plots these energy differences as functions of the parameter related to how the diffuse basis functions are scaled to generate a so-called stabilization plot (SP), an example of which is shown¹⁹ in Figure 1.

In this example, increasing Z could, for example, involve contracting the radial extent of the scaled basis. Alternatively, Z could be related to $1/R$, where R is the radius of a spherical box within which a several radial basis functions are constrained. In Figure 1, the energies that grow monotonically with Z describe discretized-continuum (DC) states involving the detached electron having the corresponding kinetic energies, and these energies increase as the radial extent of the basis is contracted.

This SP shows two energy regions within which the energy of at least one state remains nearly constant over substantial ranges of Z . Near $E = 0.5$ eV and $E = 1.3$ eV such plateau regions are seen in Figure 1 (see the blue rectangles); these are signs of metastable states that the SM is designed to address. For

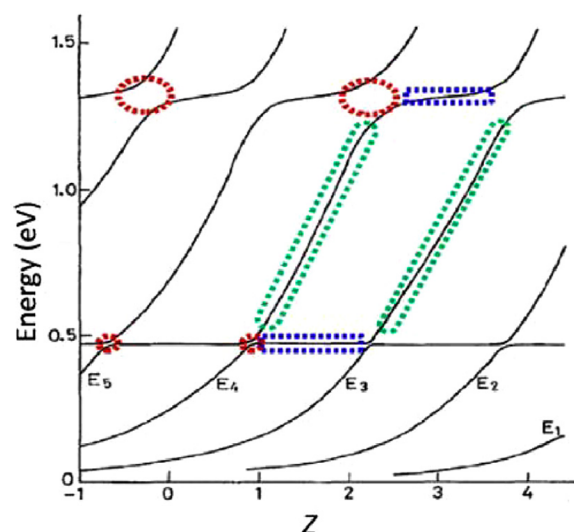


Figure 1. Generic stabilization plot showing how the energies (relative to the energy of the system in the absence of the excess electron) of several electron-attached states vary with the basis-extent scaling factor Z . Reproduced with permission from ref 19. Copyright 2018 Elsevier.

example, for values of Z between 1.0 and 2.0, the fourth lowest state's energy remains nearly constant near $E = 0.5$ eV but then undergoes an avoided crossing with the third lowest state a bit past $Z = 2.0$. In like fashion, between $Z = 2.2$ and $Z = 3.2$ a plateau occurs near $E = 1.3$ eV with avoided crossings at lower and higher Z values.

There are two differences worth emphasizing between the plateau and avoided crossings near $E = 0.5$ eV and $E = 1.3$ eV. First, the energy splittings (see the red ovals) arising in the avoided crossings are substantially larger for the metastable state near $E = 1.3$ eV than for the state near $E = 0.5$ eV. Second, the slopes of the rapidly rising DC (green) and plateau branches (blue) involved in the avoided crossings are quite different at $E = 1.3$ eV and $E = 0.5$ eV. As will be explained later, these characteristics of the avoided crossings play key roles in determining the lifetimes of the two metastable states belonging to these two plateaus.

In Figure 2, another stabilization plot²⁰ is shown in which the four lowest energies of the ${}^2\Pi_g \text{N}_2^-$ anion are shown as colored dots as functions of a basis-function scaling parameter Z , where a metastable state near $E = 2$ eV appears. In addition to plotting the four states of ${}^2\Pi_g \text{N}_2^-$, Figure 2 also shows in dashed lines three energies computed as eigenvalues of a Hamiltonian containing only the kinetic energy of the excess electron. That is, by use of the same atomic orbital basis set and the same scaling factor Z for the diffuse basis functions, but including none of the nuclei of the ${}^2\Pi_g \text{N}_2^-$ and none of the electrons of the neutral N_2 , the Hamiltonian has only the kinetic energy for the excess electron. This plot helps make it clear how the three DC levels relate to the kinetic energy of the excess electron as described by the scaled orbital basis, while the energy of the metastable state relates primarily to the valence-range character of the ${}^2\Pi_g \text{N}_2^-$. Of course, the three DC states formed in this manner with energies shown as lines are not orthogonal to the valence-type (VT) state but become orthogonalized in forming the four states' energies shown as dots.

At a value of Z near 1.2, the VT state of ${}^2\Pi_g \text{N}_2^-$ and the second DC state undergo an avoided crossing the nature of

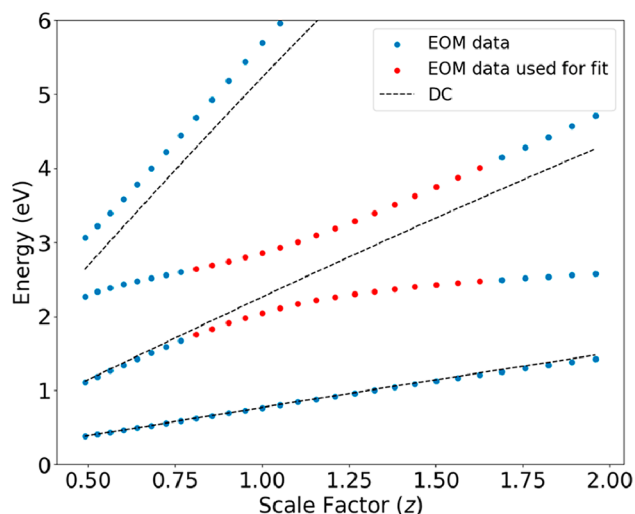


Figure 2. Three dashed lines showing the discretized-continuum states as functions of the basis scale factor Z (obtained as explained in the text by carrying out the calculation in the absence of the two N nuclei and the 14 electrons of N_2^-). The energies of the lowest four $^2\Pi_g$ states of N_2^- are shown as dots as functions of Z . Reproduced with permission from ref 20.

which I will now discuss within the lens of a simple five-parameter model.

2B. Most Basic Model for Stabilization Plot Data. In this subsection, I introduce an analytical model²¹ that embodies much of the character of the avoided crossings between one VT and one DC diabatic state occurring in many SPs and for which exact expressions can be obtained for the energy and half-width of the associated resonance state. Within this model, I show how

these resonance characteristics depend on the model's five parameters (the slopes and intercepts of the VT and DC diabatic states and their off-diagonal coupling matrix element). I also show how the precision with which these parameters can be determined depends on where within in SP one computes energy data (i.e., at what values of the scaling parameter the electronic energies are evaluated). In particular, I show that to determine the energy and half-width of a resonance to a given order of the coupling strength between the VT and DC diabatic states, one needs to utilize data points within specific ranges in the SP.

Analysis of the five-parameter model is used later in this paper to assist one in deciding where to select data points in SPs being used to create more sophisticated descriptions of how the metastable state's energy varies with the scaling parameter. By first examining the SP within the lens of the model, one can make reasonable estimates of where SP data should be computed. These estimates in turn can be used to select data points to use as input for creating more advanced descriptions (e.g., Padé rational fractions) for how $E(Z)$ depends on the scaling parameter Z . It is by this route that the insight provided by this most basic model can provide guidance when implementing the more sophisticated methods that I discuss later. I do not mean to suggest that fitting SP data to the five-parameter model can give a more accurate estimate for the resonance energy and half-width than the more advanced stabilization or extrapolation methods discussed in this paper. I only suggest that using the model can assist one in choosing Z values at which to compute the electronic energy differences $E(Z)$ used to create the SP data to use as input to the more advanced tools.

The model I now introduce was proposed in 1981 by this author and later expanded upon by Löwdin²² and improved by several others.^{23–25} In this model the diabatic energy h_1 of the

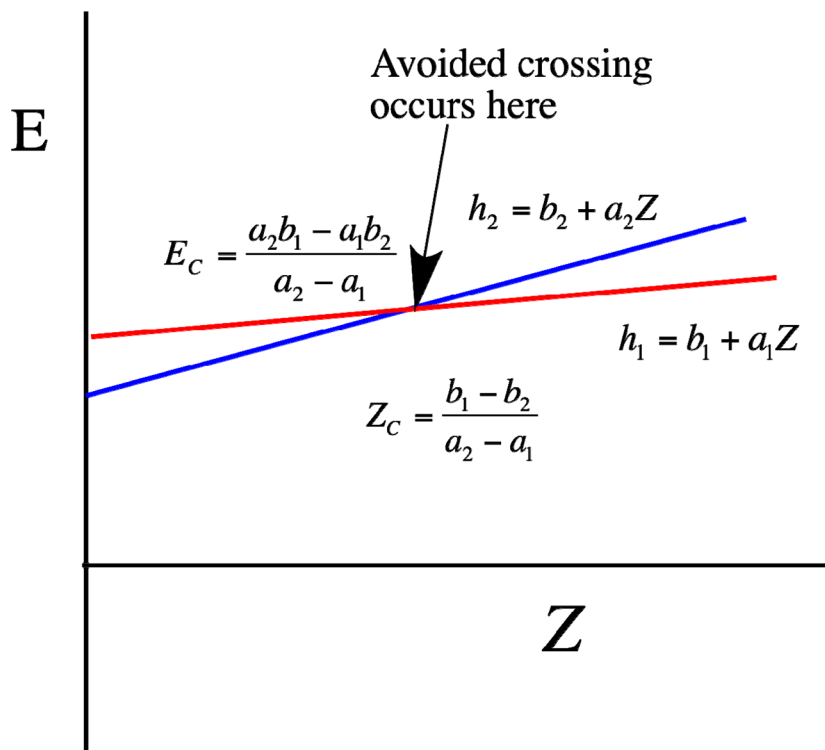


Figure 3. Plots of the diabatic VT (red) and DC (blue) energies (relative to the parent species) as functions of a scaling parameter Z showing their crossing point Z_C and crossing-point energy E_C .

VT branch of the pair of states undergoing the avoided crossing is assumed to vary linearly with the scaling factor Z as is the diabatic energy h_2 of the DC branch:

$$h_1 = b_1 + a_1Z; \quad h_2 = b_2 + a_2Z \quad (1)$$

as depicted in Figure 3. The two adiabatic states formed by coupling these two diabatic states through an off-diagonal Hamiltonian matrix element V undergo an avoided crossing near Z_C as discussed below.

Although the energies appearing in actual SPs often display significant curvatures, it can be possible to choose the scaling parameter Z to produce primarily linear behaviors in the DC and VT branches. For example, by choosing not $1/R$ but $1/R^2$ as the scaling factor when using diffuse basis functions constrained to a spherical box of radius R , the DC branches will vary nearly linearly because they will closely follow the particle-in-a-box energy expression ($k^2\hbar^2/8mR^2$). As mentioned earlier, the SP involves the differences between the energies of several of the electron-attached states and the energy of the parent species lacking the excess electron. By including the (smaller) Z dependence of the parent's energy in these energy differences, one increases the chances of obtaining (local) linear forms for the VT and DC states' energies in regions away from the avoided crossing. The energy of the VT branch is expected to be much less sensitive to the scaling that has been applied to the more diffuse basis functions, so it often has a much smaller slope a_1 than that of the DC branch a_2 . In fact, one might be tempted to expect the VT state's energy to be essentially independent of any scaling applied to the more diffuse basis functions. However, because the VT state's wave function is orthogonal to the DC states' wave functions, it does not contain only a diabatic VT character; it also contains admixtures of the diabatic DC functions. These admixtures cause the adiabatic VT state, which is what is obtained in a stabilization calculation, to acquire a nonzero slope of the same sign as found for the DC states. In the Supporting Information, I offer a more detailed analysis of this matter.

Assuming that one DC state is coupled in the avoided crossing to one VT state, the model mentioned above shows that the two assumed linear diabatic energies intersect at

$$Z_C = \frac{b_1 - b_2}{a_2 - a_1} \quad (2)$$

where they have a common energy

$$E_C = \frac{a_2b_1 - a_1b_2}{a_2 - a_1} \quad (3)$$

and give rise through a coupling V to two adiabatic energies

$$E_{\pm} = E_C + \frac{a_2 + a_1}{2}(Z - Z_C) \pm \sqrt{V^2 + \left(\frac{a_2 - a_1}{2}\right)^2(Z - Z_C)^2} \quad (4)$$

which are separated by $2V$ at the diabats' crossing point Z_C . Earlier, I showed²¹ that this function of Z has complex stationary points (i.e., where $dE/dZ = 0$) at

$$Z_{sp} = Z_C \pm 2iV \frac{\frac{a_1 + a_2}{2}}{(a_2 - a_1)\sqrt{a_1a_2}} \quad (5)$$

at which it has complex values

$$E_{sp} = E_C \pm 2iV \frac{\sqrt{a_1a_2}}{a_2 - a_1} \quad (6)$$

with the solution having a negative imaginary part being relevant to the metastable state's half-width.

If one's SP data have both the DC and VT adiabatic branches varying quite linearly far from the crossing point, one can easily determine the slope parameters a_1 and a_2 . The energy at the crossing point can be determined from where the two linear functions intersect and thus produce E_C . The energy splitting between the two adiabatic curves at Z_C can then be used as $2V$ (see eq 4), and this is enough to estimate the half-width via eq 6. This is the approach I used in my group's early work in this field, but it limited us to cases in which we could "eyeball" the two slopes and the $2V$ splitting.

If one has a SP in which the VT and/or DC energies show significant curvature, one can still try to fit the data to the model as follows. One can first carry out a least-squares fit of the sum²⁰ of the energies of the adiabatic DC and VT curves using values of Z within one of the regions where the VT curve displays a clear plateau as well as closer to an avoided crossing. This energy sum should equal the sum of the two diagonal Hamiltonian matrix elements (see eq 4)

$$E_{sum} = h_1 + h_2 \quad (7)$$

which is independent of the coupling between the two states. This fit could be performed assuming these matrix elements vary linearly, quadratically, and higher with Z , which would be especially useful if the DC or VT curve displays substantial nonlinearity. One can then, having determined $h_1 + h_2$, fit the square of the difference D between the two adiabatic energies²⁰

$$D^2 = (h_1 + h_2)^2 + 4(V^2 - h_1h_2) \quad (8)$$

again expressing this quantity in a power series in Z . This fit would contain the information about the strength of the coupling V . Such an approach was recently detailed in ref 20 where it was also shown that when the VT and DC diabatic energies vary linearly, results to those given above eqs 5 and 6 can be obtained if one were to set the a_1 slope factor to zero but allow V^2 to vary quadratically with Z still limiting the parameters to a total of five. Setting a_1 to zero often makes sense since in stabilization plots for systems with very small half-widths the variation of the VT state's energy in the plateau region is slight, which makes it difficult to assign a slope to this branch. In my current discussion, I will remain with the point of view contained in the model I introduced in 1981 which assumes a nonzero a_1 and a constant V , but in the Supporting Information, I provide further information about this approach and that followed in ref 20, both of which lead to the same final results.

Of course, it is also possible to utilize more sophisticated functional forms^{7,8,25,24} than provided by eq 4 to fit to the adiabatic DC and VT energy data. A widely used and successful approach generalizes the model introduced above by expressing the two branches of an avoided crossing within a SP as solutions of a more general quadratic equation^{7,8,26}

$$P(Z)E^2 + Q(Z)E + R(Z) = 0 \quad (9)$$

where P , Q , and R are expressed as low-order polynomials in Z . Using, for example, a least-squares fitting procedure or using as many data points as there are parameters in $P + Q + R$ to convert eq 9 into a set of linear equations⁷ for the parameters, we can use energy data E_k at various Z_k values to determine the coefficients in these three polynomials. Then, the two adiabatic energies

$E(Z)$ at any value of Z can be expressed as what is sometimes called a generalized Padé approximant (GPA) or generalized rational fraction

$$E = \frac{-Q \pm \sqrt{Q^2 - 4PR}}{2P} \quad (10)$$

This expression for E can be searched for complex stationary points Z_{sp} which, if located, can then be used to make predictions of the energy and half-width of metastable states. Clearly, this way of describing the two adiabatic states' energies is also capable of treating situations in which either the VT or DC branch's energy (or both) display nonlinear dependence on the scaling parameter Z . In fact, in ref 7 the authors used P , Q , and R polynomials of orders $[3, 3, 3]$ up to $[5, 5, 5]$ and even extended eq 9 to include terms proportional to E^3 (and thus had four polynomials) to account for the existence of a second DC state in proximity to the avoided crossing.

Although it is tempting to use P , Q , and R polynomials of high order to better fit the E_k vs Z_k data, doing so produces an expression (eq 10) that can have a very large number of complex stationary points, among which only a small number relate to the energy and half-width of the metastable states of interest. In my opinion, it is therefore useful to search for methods that contain the fewest number of parameters needed to achieve a precise fit to the E_k vs Z_k data given energy data of a reasonable specified precision. In section 2D I will say much more about this issue, but at this point I want to emphasize that one needs to consider two aspects of precision when making use of any tool for extracting resonance energies and half-widths from SPs (or when using the extrapolation methods I discuss later). The anion–neutral electronic energy differences E have precision limits that depend on various aspects of the codes used to compute them; as I explain later, I think 10^{-5} eV is a reasonable estimate for how precisely these energies can be determined, but in my later analysis I allow for the possibility that a precision of 10^{-7} eV can be achieved. In addition to these precision limits on E , one has additional uncertainty resulting from how accurately the analytical formula $E(Z)$ (e.g., eq 4, eq 6, etc.) fits the electronic energy values used as inputs. Later, I have more to say about these two issues.

2C. Using Data from Only One Branch. The approaches discussed above are often performed by using energy data from both adiabatic branches of the SP since the working equations (eqs 4 and 10) have two solutions. However, one might wonder whether it would be possible to use data from only one branch to estimate the energy and half-width of the metastable state. For example, one might have energy data on the VT adiabatic state that displays quite linear dependence on the scaling parameter until the avoided-crossing region is approached. To address the possibility of using data from only one branch,¹⁹ I expand the expressions for the two adiabatic energies given in eq 4 in powers of the interaction strength V assuming the scaling factor Z is chosen so that the SP data is in the plateau region:

$$E_1 = E_C + a_1\delta Z - \frac{V^2}{\delta a\delta Z} + \frac{V^4}{\delta a^3\delta Z^3} - \dots \quad (11)$$

$$E_2 = E_C + a_2\delta Z + \frac{V^2}{\delta a\delta Z} - \frac{V^4}{\delta a^3\delta Z^3} + \dots \quad (12)$$

where

$$\delta a = a_2 - a_1 \quad (13)$$

and

$$\delta Z = Z - Z_C \quad (14)$$

The energy E_1 describes the VT plateau, and E_2 describes the more strongly sloped DC state. Clearly, if δZ is large enough, these energies vary nearly linearly with Z and develop curvature as one gets closer to the avoided crossing point.

It is straightforward to show that the E_1 function possesses complex stationary points but the E_2 function does not and that the stationary points for E_1 depend upon at what power of V^2 the expansion in eq 11 is terminated. For example, when truncated at order V^2 , E_1 is stationary at

$$Z_{\text{sp}} = Z_C \pm \frac{iV}{\sqrt{a_1\delta a}} \quad (15)$$

while E_2 is stationary at

$$Z_{\text{sp}} = Z_C \pm \frac{V}{\sqrt{a_2\delta a}} \quad (16)$$

The complex Z_{sp} of the VT function gives rise to the following complex energy for E_1

$$E_{\text{sp}} = E_C \pm 2iV\sqrt{\frac{a_1}{\delta a}} \quad (17)$$

from which one can infer a half-width

$$\Gamma/2 = 2V\sqrt{\frac{a_1}{\delta a}} \quad (18)$$

On the other hand, the (real) stationary point of the DC branch E_2 offers no complex energy and thus no estimate of the half-width.

In ref 19, expressions for E_{sp} and $\Gamma/2$ are given for the case in which the $\frac{V^4}{\delta a^3\delta Z^3}$ term is included in eq 11; it is a bit more complicated, but its expression for $\Gamma/2$ still contains only V and the ratio $\frac{a_1}{\delta a}$, whereas the exact half-width (eq 5) depends on the ratio $\frac{\sqrt{a_1a_2}}{a_2 - a_1}$. It is important to point out that the exact, the order V^2 , and order V^4 half-width expressions become equal in the limit $|a_1| \ll |a_2|$, that is, when the SP's VT state has a much smaller slope than does the SP's DC state. As I will show later, this means that it is much easier to select appropriate Z values for creating a SP when $|a_1| \ll |a_2|$.

The above analysis suggests that it would be possible to use data from the VT branch to estimate the energy and half-width of the metastable state, but it would not be possible to use data only from the DC branch. It should be noted that this observation is not a result of truncating the expansion of the full adiabatic energy expression at order V^2 ; it has also been shown¹⁹ to hold at order V^4 .

I realize that the model upon which the results discussed above are based may not offer a highly precise fit to SP data that display substantial curvature far from the crossing point. However, the functional form embodied in this model does possess the most essential features of real SP data. Its form far from the crossing point $E_C + a_1\delta Z - \dots$ is linearly varying with Z and its form as one approaches the crossing point; the term $-\frac{V^2}{\delta a\delta Z} + \frac{V^4}{\delta a^3\delta Z^3} - \dots$ displays curvature and is suggestive of a singularity. For these reasons, I believe this model does offer useful insight into issues that arise even when using more sophisticated functional forms for how the Hamiltonian matrix

elements depend on the scaling parameter Z . In particular, any approach to extracting metastable-state energies and half-widths from E_k vs Z_k data that does not succeed when attempting to fit data generated from this simple model is unlikely to succeed when fitting more complicated E_k vs Z_k data. I therefore suggest that workers test their methods on artificial data generated from eq 4 with a range of V , a_1 , and a_2 values to see if the method can generate half-widths that are essentially “exact” or accurate to only order V^2 or V^4 . In the next subsection, I will provide an example of doing so when the powerful and widely used rational fraction form is used for $E(Z)$, but first I will overview some of the history involved when data from one branch of a SP has been used.

Several years ago, in refs 24 and 25 the workers explored using data from only the VT branch and met with modest success, but their functional forms for $E(Z)$ had two-branch character built in even though they used data only from one branch. Also, in refs 8 and 25 the workers demonstrated how one can use data from the VT branch alone, but again their functional form had two-branch character built into it. Therefore, there is considerable history supporting the point of view that data from the stable VT branch of a SP can indeed be used to extract resonance energies and lifetimes.

However, there remains the question of whether it is better to use data from both branches of a SP rather than data from only the VT branch, and a key observation about using one-branch data was made in ref 24. Those authors found that extremely high precision (10^{-12} au) energy data were needed to achieve reliable results when data from only one branch were used, whereas precision many orders of magnitude lower could yield trustworthy results when two-branch data were employed. I will have more to say about this in the following subsection as I believe it is a key point to keep in mind when seeking improvements to one-branch SM and especially in EM methods where one is of necessity dealing with data from only one branch.

From eq 11 it is clear that at large Z the VT branch's energy E is expected to vary linearly with Z (and perhaps to contain higher powers of Z if the VT branch displays curvature). The terms in eq 11 that vary inversely with $Z - Z_C$ in combination with the term varying linearly with $Z - Z_C$ suggest that a rational fraction (RF) could be a useful way to model the Z dependence of E because such functions can describe the behavior of a function at both large and small Z within a one-branch functional form. Here is an example of such an RF (often called Padé approximants):

$$E_{\text{RF}}[N, N - K] = \frac{n_0 + n_1Z + n_2Z^2 + \dots + n_NZ^N}{1 + d_1Z + d_2Z^2 + \dots + d_{N-K}Z^{N-K}} \quad (19)$$

In eq 19, an RF of power N in the numerator and power $N - K$ in the denominator is shown. Such an RF would allow the large- Z form of E to contain terms of power Z^K and lower. For example, choosing $K = 2$ would describe E varying linearly and quadratically at large Z . This approach was studied recently in ref 19 where particular focus was placed on how to select the values of Z at which to calculate the VT-branch E given a limited precision in the E values as I will discuss in the next subsection. It is worth noting as pointed out in ref 14 when studying the applications of RF functions to the extrapolation problem I discuss in section 3 that difficulties arise when extending the powers of Z beyond what the precision of the energy data can tolerate. Moreover, if the orders N and $N - K$ grow too large,

some/many of the stationary points found as solutions to $dE_{\text{RF}}/dZ = 0$ can have little or no relationship to the desired metastable-state energy and half-width.

The idea of using data only from the plateau branch of a SP and employing a RF functional form for $E(Z)$ was explored recently¹⁵ in a nice study of metastable states of the He atom and of the H_2 molecule. These workers concluded that if only data far from the avoided crossing were used, the RF was able to extract a reasonable half-width, but when data closer to the avoided crossing were included, the RF method did not succeed. In fact (see Figure 3c in ref 15), the data points used when the method failed included points spanning both sides of the avoided crossing. I note that it is not clear from that reference what numerical precision for the energy E was used in carrying out the fit to the RF function by using data far from the avoided crossing. Because the energies and half-widths obtained in ref 15 appear to agree well with results obtained by other workers using other means, it is likely that the precision to which E had been determined in ref 15 met the criteria that I will describe in the next subsection when the data were collected far from the avoided crossing.

In a more recent paper,²⁷ some of the same workers as in ref 15 revisited the issue of where to select single-branch data points in forming an RF after finding that different stationary points, and thus different energies and half-widths were obtained when data from different portions of the SP plateau (VT) branch were used to form the RF. The workers of ref 27 introduced a new so-called clustering technique aimed at identifying which stationary points are more likely to be realistic and which are likely to be artifacts. In this approach, one selects data points at Z values (α values in ref 27) from a variety of ranges within the plateau of the SP to form an RF from which resonance energies and half-widths are obtained. By examining how sensitive the resultant resonance parameters were to the location of the data points, the authors of ref 27 searched for clusters of Z values from which the resonance parameters were more consistent (i.e., had lower standard deviation). I note (see Figure 3a from ref 27) that the clusters of optimal α values identified following this route for the $\text{He}(2s^2)$ case also treated in ref 15 fall near $\alpha = 1.0$ and $\alpha = 1.6$, which are considerably closer to the avoided crossing points than where the data were taken in ref 15. This illustrates why I think it is useful to have tools for suggesting where (i.e., Z or α values) it is best to collect energy data to use in forming the Padé or any other approximants to describe a SP. I think the clustering technique offers one approach, but I suggest that the approach based on the five-parameter model as I describe in the next subsection can also be useful as I will illustrate first on data from a model for which the exact answers are known and then on data from the $\text{He}(2s^2)$ plots of refs 15 and 27.

2D. Where to Choose Z Values to Create a SP. Even when creating a SP from *ab initio* electronic energies and even when planning to use that SP to form a more sophisticated analytical expression for $E(Z)$, I suggest that first viewing the SP data within the lens of the five-parameter model can provide insight into how close to an avoided crossing one must approach when selecting Z values at which to evaluate the adiabatic energies (both E_1 and E_2 if using both branches or E_1 if using only the VT plateau).

To illustrate, for the moment assume that one is presented with a SP whose VT branch data derived from eq 4 where, of course, we know what the exact resonance energy and half-width are. The analysis offered above tells us that if only Z values far

enough from Z_0 to make the magnitude of the $\frac{V^4}{\delta a^3 \delta Z^3}$ term less than the precision ε to which the energies E are known, while rendering the $\frac{V^2}{\delta a \delta Z}$ term larger than ε , the half-width should turn out to be that given in eq 18, not the correct half-width of eq 6. The good news is that, as noted earlier, these two half-widths do not differ much if the slope of the VT branch is very much less than that of the DC branch. However, when one is faced with a VT branch of the SP that has a more substantial slope, it is important to select Z values within which the $\frac{V^4}{\delta a^3 \delta Z^3}$ term exceeds the energy precision ε as I will now illustrate.

The quantities $\frac{V^2}{\delta a \delta Z}$ or $\frac{V^4}{\delta a^3 \delta Z^3}$ exceed in magnitude the numerical precision ε to which the electronic structure code determines the energy E if

$$\delta Z \leq \frac{V}{\varepsilon} \frac{V}{\delta a} \quad (20)$$

for the V^2 term and

$$\delta Z \leq \left(\frac{V}{\varepsilon}\right)^{1/3} \frac{V}{\delta a} \quad (21)$$

for the V^4 term; analogous expressions can be obtained for having terms of higher V^2 power exceed ε . Let me now illustrate using two sets of SP data: first one with $|a_1| \ll |a_2|$ and then one with $|a_1|$ comparable to $|a_2|$.

In Figure 4, an SP is shown¹⁹ in which a metastable state near $E = 2.5$ eV appears. The two dashed curves are the two adiabatic

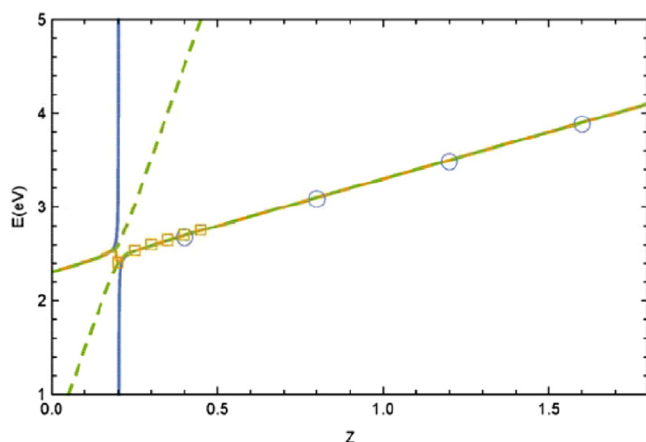


Figure 4. Two adiabatic energies (dashed line) generated from the five-parameter model showing their avoided crossing with data points (circles and squares) used to extract energies and half-widths from them. The slopes and coupling strength are given in the text. Reproduced with permission from ref 19. Copyright 2018 Elsevier.

energies; the blue line is not relevant to the present discussion. These data were generated from eq 4 by using $a_1 = 1.0$ eV/Z for the slope of the VT branch, $a_2 = 10$ eV/Z for the DC branch's slope, $V = 0.1$ eV, and $Z_C = 0.20$.

Assuming that the electronic energies are computed to a precision that generates an ion–neutral energy difference reliable to $\varepsilon = 10^{-5}$ eV, eq 21 says that one must select values of Z within 0.239 of Z_C to have precision sufficient to extract information about order V^4 . Equation 20 suggests that one can select values of Z as far as 111 units away from Z_C to be able to gain information about order V^2 .

For the SP data of Figure 4, it turns out that the slope of the VT branch is sufficiently less than the slope of the DC branch that the exact, V^2 , and V^4 level half-widths are very similar: 0.0703, 0.0667, and 0.0697 eV, respectively. Therefore, in this case it would be safe to use data at values of Z quite far from the avoided crossing because obtaining a half-width of V^2 quality would be sufficient. However, when the slopes of the two branches are closer in magnitude, things are very different as I will now illustrate.

Now, assume one were to use $a_1 = 4.0$ eV/Z for the slope of the VT branch, $a_2 = 6$ eV/Z for the DC branch's slope, $V = 0.1$ eV, and $Z_C = 0.20$ to generate SP data from eq 4. Note that this case differs from the one treated above not in the strength of the coupling V or in the energy of the resonance but only in the VT and DC slopes. Equation 21 tells us, again assuming an energy precision of $\varepsilon = 10^{-5}$ eV, that one would need to select data points (at least five of them given the model has five parameters) no farther than 1.08 from Z_C to obtain a half-width of V^4 accuracy; to achieve a half-width of V^2 accuracy, eq 20 says Z can be as far from Z_C as 500. In this case, there are very large differences among the exact, V^2 , and V^4 level half-widths; they are 0.4899, 0.2828, and 0.3810 eV, respectively. Thus, for such a case it is important to know at what Z values to compute the energies if one wants to achieve the best results.

To examine to what extent the guidance provided by analyzing the SP data in the lens of the five-parameter model is useful when creating a Padé representation of such data, we created a [3, 2] Padé representation for the data set discussed immediately above and used six Z values (this Padé has six parameters as seen in eq 19): $Z = 0.4, 0.6, 0.8, 1.0, 1.2,$ and 1.4 . Notice that five of these six Z values fall within the $\delta Z < 1.08$ criterion to achieve a V^4 level half-width, but the sixth Z value is outside this range. However, this Padé fit produced a half-width of 0.287 eV, close to the V^2 level result but not close to the V^4 level result. Even by extending our Padé representation to [4, 3], [5, 4], and [6, 5] by using the six above-specified Z values and additional Z values above $Z = 1.28$, essentially the same V^2 level half-width was obtained. This shows that even a high-order Padé equation cannot go beyond the precision of the energy data that it is given as input, which is one of my main points.

The good news from this numerical experiment is that the [3, 2] (or higher) Padé representation of the SP data generated by using $a_1 = 4$ and $a_2 = 6$ works very well if one uses six or more data points *all* within $\delta Z < 1.08$. For example, when these six Z values are used, 0.25, 0.40, 0.55, 0.70, 0.85, and 1.00, a half-width of 0.4892 eV is obtained, which is very close to the exact half-width. I hope this illustrates how it can be useful to first examine SP data within the lens of the simple model (i.e., attempt to estimate the two slopes and the coupling parameter V) and to then use eqs 20 and 21 to assist in deciding where to focus energy data used in generating a Padé (or other sophisticated) expression for $E(Z)$. As with the clustering strategy discussed earlier, this path offers a way to focus on the most important region(s) within the SP's VT branch.

Now, let me illustrate how this strategy applies to the He($2s^2$) data of refs 15 and 27 where the exact results are not known but for which highly accurate results from other methods are presented. Taking the SP data of Figure 2 in ref 27, which is essentially the same as the SP data shown in Figure 3a of ref 15, I estimated the slope of the VT branch to be $a_1 = -0.015$ and the slope of the other branch to be $a_2 = -2.00$ (both having units of hartree per unit change in α). From this same SP, I estimated the splitting between the two adiabatic states at the avoided crossing

point to be $2V = 0.0375$ hartree. I then used these values with the simple model I cite in the paper to estimate how close $\delta\alpha$ to the avoided crossing point one must collect data assuming that the electronic energies are precise to $\varepsilon = 10^{-5}$ eV = 3.7×10^{-7} hartree and assuming one wants to achieve results of V^4 level (see eq 21). This produced $\delta\alpha = \frac{V}{a_2 - a_1} \left(\frac{V}{\varepsilon}\right)^{1/3} = 0.35$. From the SP in Figure 2 of ref 27, one can see that the crossing point occurs at ca. $\alpha = 0.8$, so this means that data points should be focused in the region not beyond $\alpha = 1.15$ according to eq 21. I note that this suggestion is very much in line with the results obtained by using the clustering method as shown by the data points contained within the red circle in Figure 3a of ref 27. I hope this example and the two shown earlier for the model data where the exact answers were known support my claim that using the simple model put forth here can be useful in deciding at what values of the scaling parameter one should focus computed E values.

I should note that the utility of the strategy I just outlined is, of course, limited by (i) the extent to which one can estimate V from the energy splitting and (ii) the extent to which one can estimate the slope difference $a_2 - a_1$ and the degree to which the two branches of the SP display linear behavior away from the crossing point. Using $\varepsilon = 10^{-5}$ eV in eq 21, the expression for $\delta\alpha$ reduces to $\delta\alpha = 46.4 \frac{V^{4/3}}{a_2 - a_1}$ with V and the slope parameters expressed in eV and eV per unit of α , a result that can be used to estimate the uncertainty in $\delta\alpha$ given uncertainties in V and in $a_2 - a_1$.

In the above analysis, I used $\varepsilon = 10^{-5}$ eV as a reasonable estimate of the precision to which the ion–neutral energy difference can be obtained. I realize that most modern electronic structure programs use double (or higher) precision arithmetic, evaluate the one- and two-electron integrals to precisions better than 10^{-5} eV, and have convergence and matrix eigensolver routines that are of very high precision. Nevertheless, even when attempting to carry out a calculation by using the same basis set and the same level of electron correlation (e.g., Hartree–Fock, MP2, CCSD(T), EOM-CC, etc.), there can be slight differences among research laboratories (e.g., self-consistent field convergence, eigenvalue solver routines, geometry optimization algorithms, solving the EOM-CC equations for several roots, etc.) that cause the final energies to vary by ca. 10^{-5} eV from one research lab to another. So when one uses energy values generated by the electronic structure code to many figures beyond 10^{-5} eV, the resulting RF might offer a good fit to the data but the data themselves and the resultant RF are still not trustworthy to better than 10^{-5} eV.

Finally, I also note that methods that use the total electronic energy of the electron-attached system under study are even more prone to the issue of limited precision because such total energies are extensive quantities and become very large in magnitude as the molecular size increases. To compute the anion–neutral energy differences used to form the SP, one has to subtract two such large numbers, which adds to the energy uncertainty. In contrast, methods such as Koopmans' theorem and Green's function or equations of motion methods are less prone to this problem because they evaluate the intensive electron binding energy directly.

Although these points are made in context of discussing using one-branch VT data within stabilization methods, they are going to appear again in section 3 when I discuss how one should be

aware of the precision to which E values are computed when using the extrapolation methods discussed there.

3. EXTRAPOLATION METHODS

3A. A Different Type of Stabilization Plot. In these approaches one adds to the system's electronic Hamiltonian a potential V_{att} that is differentially attractive in regions where the core and valence electrons reside and one computes the electronic energy at various strengths ZV_{att} of the added potential. If the strength factor Z is large enough, the modified Hamiltonian will produce a bound electronic state. For values at this and higher Z , the electronic energy can be computed by using conventional bound-state methods. For example, as explained earlier, in studying¹⁸ SO_4^{2-} , one could change the charge on the sulfur nucleus to be $16 + Z$; if Z were to equal 1.0, the calculation would correspond to one on the ClO_4^- anion which is electronically bound. By finding the smallest value of Z that renders the system bound and then carrying out a series of calculations at this and higher values of Z , one can generate energy data to be used in an extrapolation method (EM). For example, one might posit to fit the $E(Z)$ data to a low-order polynomial in Z and to then extrapolate back to $Z = 0$. However, the more successful EMs have made use of knowledge about how the function $E(Z)$ should behave in the region where E moves from negative (i.e., describing a bound state) to positive and have shown that such a polynomial representation is not appropriate. Incorporating this aspect of the functional form has proven to be a key component of the more successful EMs as I will now describe.

One potential advantage of the EM approaches is that one can utilize electronic structure methods that focus on only one (e.g., the lowest energy) state in determining the energy of the VT state once it has been sufficiently stabilized. Therefore, for example, high-level methods such as CCSD(T) can be used. However, one still has to compute such an energy for both the electron-attached and neutral parent species to obtain the energy difference used as input to forming a Padé or other representation.

Now, I want to show the results¹⁶ of a calculation in which a stabilizing potential has been added to generate the kind of data discussed above. But I want to show how the energies of the DC states also evolve when the added potential acts because doing so illustrates one of the difficulties that arise when certain stabilizing potentials are used. To do so, I selected a set of calculations from ref 16 in which the authors used a multistate configuration interaction method so they could simultaneously determine the energies of the VT and DC states. In Figure 5, I show such a plot pertaining to the lowest metastable shape resonance of CO_2^- . Note that the strength parameter ξ is defined to begin at $\xi = 1$ (thus corresponding to $Z = 0$ in my notation) as I have to correct for this difference in the following discussion.

The energies (anion–neutral energy differences) shown in blue are those in which the ground electronic state of the CO_2^- anion has become bound and have been used as input data in ref 16 to form a Padé representation; the six other red curves describe how the DC states in this calculation on CO_2^- evolve as the potential acts to differentially stabilize the VT state. Clearly, the DC states are also being stabilized but not as much as the VT state.

In all of the EMs I know of only energy data taken from the region in which the VT is electronically bound are used to carry out the extrapolation. In other words, even though the workers

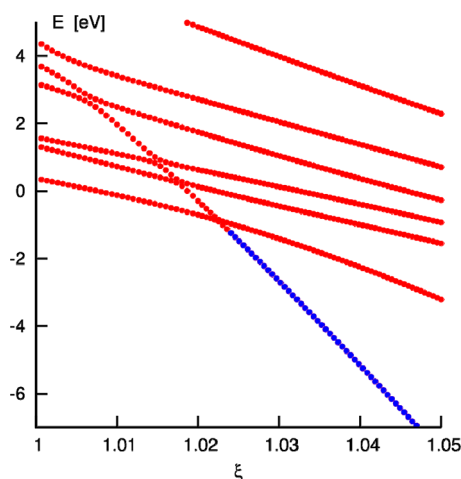


Figure 5. Plots of energies for the shape resonance state of CO_2^- for the stabilized VT state (blue for $\xi > \text{ca. } 1.022$ and continuing red for ξ below that) and DC states (other red) as functions of the strength ξ of the stabilizing potential. Reproduced with permission from ref 16. Copyright 2015 AIP Publishing.

of ref 16 examined how the energies of several DC states varied as the strength of the stabilizing potential was changed, they only used data (the blue points) taken from the bound-state VT data. In that study, the workers examined the behavior of the DC states because they wanted to emphasize how certain stabilizing potentials V_{att} gave rise to unwanted effects on the DC states whereas the shorter-range potentials they prefer were less problematic. I emphasize this so the reader understands that EM methods usually do not look for avoided crossings between VT and DC states; they only look at the character of the VT state once it has become bound. Therefore, it is important to keep in mind that unlike when using SP methods, one does not have two states whose avoided crossing magnitude can be used to estimate the coupling strength V ; one only has a plot of the VT state's energy in the region where it is stable.

3B. Problem with Intervening Rydberg-like States.

Before describing the EMs that have been used to extrapolate the

kind of data shown in blue in Figure 5 to obtain the energy and half-width of the corresponding metastable state, I want to point out a problem that can and often does arise in this kind of study as the workers in ref 16 addressed. Notice that for values of the strength factor (ξ in Figure 5) greater than ca. 1.007 the lowest DC state's energy has dropped below zero. Notice also that this DC state's energy is actually below that of the differentially stabilized VT state for values of ξ up to ca. 1.022. Therefore, any electronic structure method that is focused on locating and characterizing only the lowest bound state of a given symmetry would not find the VT state in this range of ξ . This is a problem because it limits one's ability to follow the evolution of the desired VT state from large values of ξ downward to where the energy of the VT state crosses $E = 0$.

It is the long-range character of the differential stabilizing Coulomb potential $V_{\text{att}} = \frac{-\xi}{r}$ used to generate the data in Figure 5 that causes the DC states' energies to undergo substantial stabilization and, for several of these DC states, to drop below $E = 0$ as ξ increases. In effect, these DCs evolve into Rydberg-like states at larger ξ values, and in ref 17 we are reminded that this danger in using a purely Coulomb stabilizing potential can be difficult to overcome. In ref 16 and again by other workers in ref 17 it is shown that using an attenuated Coulomb attractive potential can help overcome this difficulty and can do so with little modification to the one-electron integral codes contained in most *ab initio* electronic structure programs. In ref 7 a stabilizing potential that is constant ($-q/R$) inside a sphere of radius R and Coulomb-like ($-q/r$) outside the sphere was employed along similar lines. Other workers²⁸ have used dielectric stabilization to render the VT state bound, but these same workers have not utilized such E data to attempt to compute the half-widths.

Another example of how Rydberg-like states arise in such studies²⁹ when using the pure Coulomb potential to effect the differential stabilization is shown in Figure 6. Here we see the energy (here by using $E > 0$ to denote a bound state) of the $^2\Pi_u$ diacetylene $\text{H}-\text{C}\equiv\text{C}-\text{C}\equiv\text{C}-\text{H}^-$ anion at the equilibrium geometry of the neutral (relative to its neutral) evolves as the charge λ added to each of the six nuclei is increased. For values of

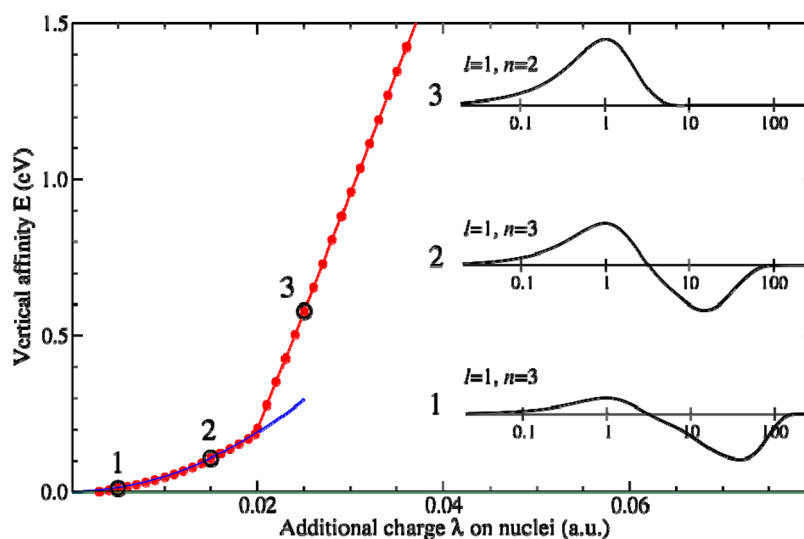


Figure 6. Plots of the energies of the stabilized $^2\Pi_u$ VT state of diacetylene anion (line including point 3) and in intervening Rydberg-like state (curve containing points 1 and 2) as functions of the strength parameter λ . Also shown is the radial dependence of the lowest-energy state at data points 1, 2, and 3. Reproduced with permission from ref 29. Copyright 2015 AIP Publishing.

$\lambda > 0.02$, the lowest energy state is the desired VT state of the anion. But as λ decreases below 0.02, a Rydberg-like state becomes lower in energy than the VT state. This causes problems in extrapolating the VT state's energy to find the point where it crosses $E = 0$ which, as I explain below, is important to know when using EMs. These plots of the radial component of the singly occupied molecular orbital as functions of the distance from the center of the molecule at the three data points indicated in Figure 6 amplify the issue. At data point 3, the radial function has a single lobe with a maximum near 1.0 Å and is characteristic of a diacetylene π^* VT orbital, but at points 1 and 2 it extends to much longer distances as expected for a Rydberg-like orbital.

Another feature of the Rydberg-like state's energy that is worth noting is its quadratic dependence λ^2 on the coupling constant, whereas the stabilized VT state's energy varies nearly linearly with λ in Figure 6. It turns out, as I discuss later, that these different λ dependences are important to keep in mind when deciding what kind of stabilizing potential to use in performing extrapolation studies. Potentials of the Coulomb form $V_{\text{att}} = \frac{-\xi}{r}$ that are singular at $r \rightarrow 0$ are most prone to the difficulties involving spurious Rydberg-like states as discussed in refs 16 and 17.

Before moving on to describe how one makes use of the data from the electronically stable portion of the plots shown in Figures 5 and 6, I want to emphasize that this kind of plot is very different from the SPs used in the stabilization method described earlier even though they both have avoided crossings between VT and DC (or Rydberg) branches. In one case, the key features are the plateau behavior of the branch describing the VT character of the metastable state and the avoided crossings this plateau branch undergoes with DC branches whose energies intersect its plateau energy. In the second case, the key features are the behavior of the VT state that has been rendered bound by the differentially stabilizing potential and the functional form of $E(Z)$ that can be used to extrapolate back to $Z = 0$. The avoided crossings between the VT branch and the DC branches in the latter class (Figure 5 shows five of these) do not play the same role as in the first class of SPs. For example, the avoided crossings near 1.2 and 2.7 eV are not to be used to say anything about the half-width of the CO_2^- metastable state; only the behavior of the VT branch near $\xi = 1.0$, where E is ca. 4 eV, can be so used, and this behavior is obtained only via extrapolation of the EM formula $E(\xi)$.

3C. Most Basic Extrapolation Formula. A key concept underlying the formulas used to extrapolate the $E(Z)$ data from the bound state where $E < 0$ (returning to our earlier convention) into the unbound and potentially metastable region where $E > 0$ lies in understanding how the momentum p of the ejected electron evolves as one moves through $E = 0$. For $Z > Z_1$, this critical value, the momentum, is purely imaginary because $\frac{p^2}{2m_e} = E$ is negative (i.e., as for a bound state). Moreover, it is known that for a state of nonzero angular momentum (e.g., the $^2\Pi_g$ shape resonance of N_2^-) this momentum approaches and passes through zero in the following manner:^{3,11,30,32}

$$p = i[-a + b\sqrt{Z - Z_0}] \quad (22)$$

Hence, for $Z < Z_0$ the momentum develops a real component and becomes

$$p = i[-a \mp ib\sqrt{Z_0 - Z}] \quad (23)$$

These constraints on how the momentum varies near $E = 0$ then suggest how the energy itself should vary (assuming atomic units in which $m_e = 1$) as

$$E = -\frac{1}{2}a^2 - \frac{1}{2}b^2(Z - Z_0) + ab\sqrt{Z - Z_0} \quad \text{for } Z \geq Z_0 \quad (24)$$

and

$$E = -\frac{1}{2}a^2 - \frac{1}{2}b^2(Z - Z_0) - iab\sqrt{Z_0 - Z} \quad \text{for } Z \leq Z_0 \quad (25)$$

The functional form given in eq 24 suggests that E should be real and decrease linearly with Z at large Z having a slope of $-1/2 b^2$ and should pass through $E = 0$, $Z = Z_0 + a^2/b^2$. Once Z drops below Z_0 , E develops an imaginary component that grows in magnitude until it reaches $-iab\sqrt{Z_0}$ at $Z = 0$. In this same range, the real part of E should increase linearly with slope of magnitude $1/2 b^2$ as Z decreases to $Z = 0$. In Figure 7, I show an

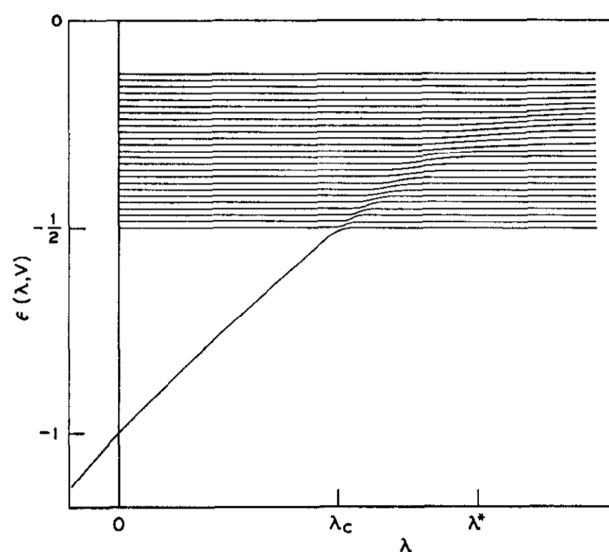


Figure 7. Plots of the energies (in atomic units) of the destabilized VT state of H^- having a variable nuclear charge (see text) and of numerous DC states (horizontal lines) as functions of the strength parameter λ . Reproduced with permission from ref 31. Copyright 1966 AIP Publishing.

EM plot³¹ (using ϵ for E and λ for Z) to illustrate this kind of behavior. The energies shown here are those of a two-electron atom having a nuclear charge that is reduced from $Z_{\text{Nuc}} = 2.0$ by an amount described by the parameter λ . As λ increases and approaches λ_c , the energy approaches that of a neutral H atom ($-1/2$ au) and a free electron of zero kinetic energy. For even smaller values of the nuclear charge, the two-electron system has a metastable state that is treated by using a SM type method detailed in ref 31.

In Figure 7, an increase in λ should be interpreted as a decrease in the nuclear charge and $\epsilon = -1/2$ au should be interpreted as $E = 0$. Moreover, the multitude of horizontal lines are to be viewed as a multitude of DC states that approximate the continuum of a H atom plus a free electron. The plot shows how the bound state's energy varies (essentially) linearly when the strength parameter is large and how the energy evolves into the continuum once E crosses 0; this is analogous to what is shown in Figure 5.

The most important lesson from the discussion thus far is that the functional form^{3,8,10,32} for how E depends on Z cannot contain only powers of Z (or of $Z - Z_0$); it must contain powers of $\sqrt{Z - Z_0}$ if it is to be capable of extrapolating to $Z = 0$ in a manner that can produce a complex E and thus a proper half-width. The expressions in eqs 24 and 25 are the most elementary form that has been used, but much progress has been made in developing more rigorous and reliable equations for $E(Z)$ to use as I will now discuss.

3D. More Sophisticated Extrapolation Formulas. I begin by emphasizing that the EMs used in the context discussed here involve using data from a stabilization plot containing only the VT state's energy; one wants to use data where the VT state of interest is bound and to then extrapolate the data for only this branch back to $Z = 0$ to predict the complex E that corresponds to the metastable state. This should remind the reader of the earlier discussion of using data from one branch of a stabilization plot of the standard SM. However, these two situations are quite different. In the present case, the branch one follows describes the VT state's energy that has been stabilized (lowered) through application of the additional attractive potential V_{att} and this branch has a higher slope than do the DC branches. In the traditional SM plot, the branch one follows, if one is attempting to use data from a single branch, is the plateau of the VT state, and in this case, the branch has a smaller slope than do the DC branches.

Even though the branches one is attempting to describe in the present (EM) and earlier (SM) cases differ substantially as just explained, they have some characteristics in common, and these characteristics help guide the formation of more sophisticated functional forms for $E(Z)$ than that given in eqs 24 and 25. They both often vary (approximately) linearly for values of Z far from some critical point (Z_C in the SM case and Z_0 in the EM case), and they both have slopes that decrease significantly in magnitude as one approaches the critical point. These observations as well as the essential observation that one must use powers of $\sqrt{Z - Z_0}$ rather than powers of Z when performing extrapolations suggest that rational fractions involving $\sqrt{Z - Z_0}$ analogous to eq 19 should be capable of providing reliable extrapolation tools; indeed, this has turned out to be true.

In the region where the VT state being followed is bound, the anion's energy lies below that of the neutral so E is negative. But

$$\frac{p^2}{2} \equiv -E \equiv \kappa^2 \quad (26)$$

can be used to define a (artificial) momentum p (or as some workers prefer κ) in terms of the square root of the positive quantity $-E$. Given a set of (real) κ_i values each computed at a set of Z_i , an RF of the form

$$\kappa_{\text{RF}}[N, N - K] = \frac{n_0 + n_1 y + n_2 y^2 + \dots + n_N y^N}{1 + d_1 y + d_2 y^2 + \dots + d_{N-K} y^{N-K}} \quad (27)$$

can be formed with the expansion being in powers of

$$y = \sqrt{Z - Z_0} \quad (28)$$

if one has a way to find the value of Z_0 , which I will discuss shortly. A set of (real) κ_i values ($\kappa_i = \sqrt{-E_i}$) computed at a set of (real) $y_i = \sqrt{Z_i - Z_0}$ values can be used to determine the n_i

and d_j coefficients in the RF. Then, the RF can be evaluated at $Z = 0$ (i.e., at $y = i\sqrt{Z_0}$ to, via eq 27, generate the complex value of $\kappa_i = \kappa_i + i\kappa_i$. The complex energy is then given as

$$E = \kappa_i^2 - \kappa_r^2 - 2i\kappa_i\kappa_r \quad (29)$$

To implement this approach, one must be able to compute the $y_i = \sqrt{Z_i - Z_0}$ quantities for each Z_i , which requires knowing Z_0 . This can be approximated by first extrapolating the data computed for the electronically bound state to $E = 0$ to find an approximate Z_0 and then proceeding to use this Z_0 to calculate the $y_i = \sqrt{Z_i - Z_0}$, but if Rydberg-like states intervene as in Figure 6, this extrapolation can be of limited accuracy. In ref 16, it is suggested that an iterative process for determining Z_0 can also be used.

There are several methods that have proven useful in determining the n_j and d_j coefficients from the κ_i and y_i inputs. In refs 12 and 13 a least-squares procedure is outlined and implemented with good success. In ref 17 the authors suggest using a method developed by Schlessinger³³ in which a truncated continued fraction is recursively formed by using these same inputs.

To illustrate the success in using the kind of EM method outlined above, I note that in ref 12 some of the pioneers of this approach used [1, 1] through [4, 4] RFs to study metastable ${}^2\Pi_g$, N_2^- and found that a [3, 3] RF was sufficient to achieve reliable results. I mention this to make it clear that experience has shown that one does not have to employ RFs of very high order because the most important ingredient to forming the extrapolation formula is to use $y = \sqrt{Z - Z_0}$ as the independent variable. A [2, 1] RF contains four coefficient parameters, a [3, 2] has six, and a [4, 3] has eight.

However, there are significant challenges to employing the kind of extrapolation formulas discussed above. To illustrate, I show in Figure 8 plots of the stabilized VT state of the ${}^2\Pi_u$

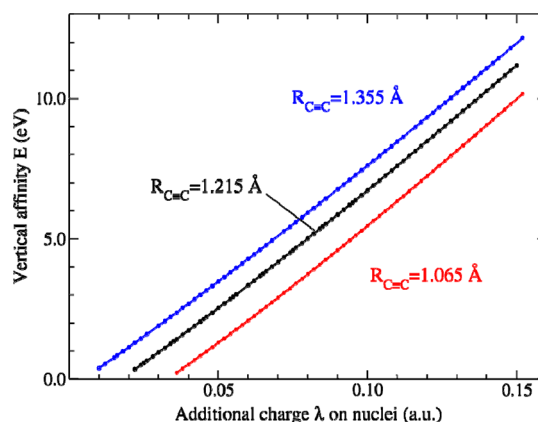


Figure 8. Plots of the energies of the stabilized VT state of the diacetylene anion at three bond lengths as functions of the strength parameter λ . Reproduced with the permission from ref 29. Copyright 2015 AIP Publishing.

diacetylene anion²⁹ at three different C≡C bond lengths. In these plots positive energy corresponds to an electronically bound anion, and λ is the amount of extra charge added to each of the six nuclei in the molecule to generate the stabilizing Coulomb potential.

It should be clear that for each of the three bond lengths the SP data vary nearly linearly with λ in the region within which the

anion is bound, especially at large λ . Reflecting back on what was said in section 2D about attempting to follow a plateau region of a SM SP toward the avoided crossing region, one should expect that energy data of high accuracy will be needed in this case as well. That is, even if the extrapolation formula has the correct analytical form to permit it to be used to extrapolate E data from the region where the anion is stable toward $\lambda = 0$, the terms in the formula that contribute to the half-width in particular will be very small in the large λ range of E values (since the linear variation dominates here) which is why high-precision E data are needed. This point is amplified in Figure 9 where I show the results obtained (real part of E and full width Γ) obtained in ref 12 in their study of ${}^2\Pi_g N_2^-$.

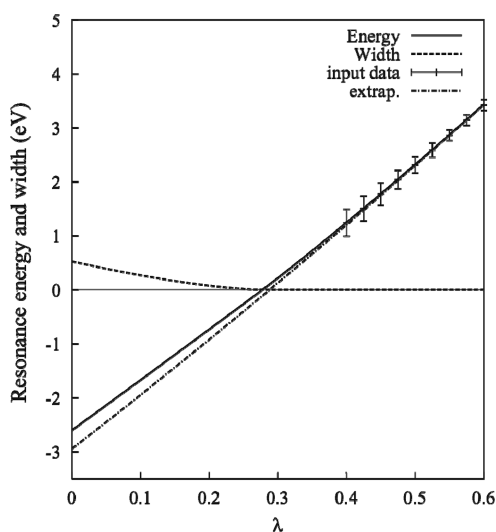


Figure 9. Plots of the energies and half-widths of the VT state of ${}^2\Pi_g N_2^-$ as functions of the strength parameter λ ; see text for details. Reproduced with permission from ref 12. Copyright 2010 AIP.

In Figure 9, the nine energy data points used to form the RF and to then do the extrapolation are shown where one can see that they very closely follow the linear plot labeled “extrap”. The authors of ref 12 can compute the real part of the resonance energy and half-width at various values of the stabilizing potential’s strength λ by evaluating the RF (eq 27) at various values of $y = i\sqrt{\lambda_0 - \lambda}$. Therefore, the RF used to fit these data points produces a function $E(\lambda)$ (labeled “Energy”) that (i) remains real down to ca. $\lambda = 0.3$, after which it becomes complex with (ii) its real component evolving down to ca. $E = -2.5$ eV at $\lambda = 0$ and (iii) twice its imaginary part Γ (labeled “Width”) evolving from 0 at $\lambda = 0.3$ to ca. 0.5 eV at $\lambda = 0$.

More recently, a variant of the RF extrapolation approach described above developed by many of the scholars who pioneered the approach just described has proven to be even more effective. It is based on the observation²⁹ that when $\kappa = \sqrt{-E}$ varies with Z as

$$\kappa \propto \sqrt{Z - Z_0} \quad (30)$$

the inverse function must vary as

$$Z \propto Z_0 + a\kappa^2 \quad (31)$$

meaning that $Z(\kappa)$ must be an increasing function κ with a local minimum at $\kappa = 0$. Therefore, instead of expressing κ as a RF in

powers of $y = \sqrt{Z - Z_0}$, the authors of refs 14, 29, and 34 proposed to express Z as a RF in powers of κ

$$Z_{\text{RF}}[N, N - K] = \frac{n_0 + n_1\kappa + n_2\kappa^2 + \dots + n_N\kappa^N}{1 + d_1\kappa + d_2\kappa^2 + \dots + d_{N-K}\kappa^{N-K}} \quad (32)$$

Using a set of E_j computed at Z_j where the electron-attached species is bound, the corresponding (real) $\kappa_j = \sqrt{-E_j}$ values are computed. These Z_i and κ_j are then used (e.g., employing least-squares or Schlessinger fitting³³ mentioned earlier) to determine the n_j and d_j coefficients in the RF of eq 32. Extrapolating this function to $Z = 0$ amounts to finding (complex) values of κ at which the numerator of the RF vanishes. The fact that this approach reduces the key step (finding zeros of a polynomial which can be done analytically for quadratic or cubic polynomials) to one that is quite amenable to stable numerical methods is a main reason underlying this EM’s success. The complex κ values that cause the numerator to vanish can then be used as in eq 29 to generate complex energies that might describe the metastable state’s energy and half-width. In addition to finding this approach more numerically stable than that contained in eq 27, it avoids having to find the Z_0 value needed to compute the $y_k = \sqrt{Z_k - Z_0}$ values that appear in the earlier approach. It can be seen from eq 31 that Z_0 will be determined to be n_0 (i.e., the lead term in the numerator) during the data-fitting process.

More recently, the authors of ref 29 have introduced rather clever expressions for the RF functions they use by constraining the n_k and d_k coefficients in eq 32 to ensure that the condition $Z \propto Z_0 + a\kappa^2$ is met. For example, a [2, 1] RF they use is of the form

$$Z(\kappa) = Z_0 \frac{\kappa^2 + 2\alpha^2\kappa + \alpha^4 + \beta^2}{\alpha^4 + \beta^2 + 2\alpha^2\kappa} = Z_0 + \frac{\kappa^2}{\alpha^4 + \beta^2 + 2\alpha^2\kappa} \quad (33)$$

The numerator has two complex zeros at

$$\kappa = -\alpha^2 \pm i\beta \quad (34)$$

which predict the metastable state’s energy to be

$$E = \beta^2 - \alpha^4 \quad (35)$$

and its half-width to be

$$\frac{\Gamma}{2} = 2\alpha^2\beta \quad (36)$$

This [2, 1] RF contains only three parameters Z_0 , α , and β which has been shown (ref 29) to somewhat limit its accuracy. As a result, higher order RFs, including a new [3, 2] RF of the form

$$Z(\kappa) = Z_0 \frac{(\kappa^2 + 2\alpha^2\kappa + \omega)(1 + \delta^2\kappa)}{\omega + (2\alpha^2 + \delta^2\omega)\kappa + \tau\kappa^2} \quad (37)$$

were invented^{29,34} and found to be more reliable. The above [3, 2] RF contains five parameters. A somewhat simpler [3, 1] RF containing four parameters (eq 37 with $\tau = 0$) was also shown to be reliable in ref 34.

Finally, in ref 34 it was again emphasized that when using stabilizing potentials that are singular at $r \rightarrow 0$ (e.g., a Coulomb potential or even an attenuated Coulomb potential), Z turns out to not vary as $Z \propto Z_0 + a\kappa^2$ for large κ as it should but instead varies linearly with κ , which should offer further caution in choosing the functional form^{16,17} to use for the stabilizing

potential. This linear relationship between Z and κ is what causes the energy $E = -\kappa^2$ to vary quadratically with Z in the Rydberg-like intruder states discussed earlier. In ref 34 it is mentioned that the functional form shown in eq 37 is designed to accommodate the linear variation of Z with κ at large κ and thus to be more appropriate to use if one decides to employ, for example, a Coulomb or attenuated Coulomb stabilizing potential. However, it is not clear to me that using an RF such as eq 37 that varies linearly at large κ is a good idea; doing so would seem to accommodate the intrusion of Rydberg-like states. It might be better to use a stabilizing potential that is not singular so Rydberg-like states do not arise in the first place or to choose an orbital basis set that does not produce DC states having very low energies that can change into Rydberg-like states under the influence of the singular potential.

4. SPECULATION AND SUGGESTIONS

I wish to now offer constructive suggestions that I hope workers in developing the stabilization and extrapolation fields will explore. I simply do not currently have access to the resources needed to carry out these studies, or I would do so myself. Some of my suggestions involve using data generated from eq 4 to test SM methods. I think this is useful because one knows the exact answer in this case. If a proposed SM is not capable of handling data in such an ideal situation (i.e., having two linear asymptotes and a constant coupling strength), it is unreasonable to expect it can handle more complicated situations.

- I think it is imperative when testing one's SM or EM working equations that one employ energy data accurate to no better than between 10^{-5} and 10^{-7} eV because this is likely the most precision one can expect from *ab initio* calculations of electron binding energies. This might sound like an obvious or even trivial suggestion, but it is my impression that many of the studies to date in these two areas have utilized energy data of substantially more figures. I think it is proper to determine whether the success of any method requires data that is beyond what is reasonably available.
- I suggest that one utilize (artificial) energy data (precise to only 10^{-5} or 10^{-7} eV) generated by using eq 4 (the simple model discussed early in this paper that contains five parameters) with $V = 0.1$ eV, $Z_0 = 0.200$, $E_C = 2.50$ eV, $a_1 = 4$, and $a_2 = 6$ within the working equations of one's VT-branch SM. In particular, using data only from the VT branch (the one with slope of 4), one should explore how the resultant half-widths vary as functions of (i) how many data points one uses to fit to one's SM formula, (ii) how close/far the data points are from Z_0 , and (iii) how many parameters one incorporates into one's working equations. In my opinion, a method that succeeds only by using data more precise than 10^{-5} eV is likely to be of limited use in practical calculations of metastable states.
- When considering real SP data in which two branches are clearly identified, I think it would prove useful to estimate the difference in the two (VT and DC) slopes $\delta\alpha$ and the splitting $2V$ between the two branches near the crossing point and to then use $\delta Z \leq \frac{V}{\epsilon} \frac{V}{\delta\alpha}$ and $\delta Z \leq \frac{V}{\epsilon} \frac{V}{\delta\alpha}$ (with $\epsilon \approx 10^{-5}$ eV) to estimate the range of Z values within which one should obtain energy data. I realize that these formulas derive from the most basic model of an avoided crossing as discussed earlier, but I think they can be of use

in focusing data generation within regions that are likely most important.

As detailed in the Supporting Information, I have not been able to come up with an analogous approach for locating data generation when using the extrapolation methods but I encourage others to try.

- I showed in Figure 5 an EM plot in which the evolution of the stabilized VT energy was followed in the electronic structure calculation into the region where the VT curve undergoes a series of avoided crossings until it reaches ca. $E = 4$ eV at $Z = 0$. Notice in Figure 5 how the energy splittings in these avoided crossings (just above $E = 0$, near $E = 1$ eV, near $E = 3$ eV, and finally near $E = 4$ eV) increase as one progresses upward in energy.

Equation 25 suggests that the half-width should vary with Z as $ab\sqrt{Z_0 - Z}$, and eq 6 tells us the prefactor should be proportional to the coupling strength V . It would be interesting to determine whether the series of splittings mentioned above follow the $\sqrt{Z_0 - Z}$ trend suggested by eq 25.

Within this same line of thought, the factor $2V \frac{\sqrt{a_1 a_2}}{\delta a}$ that governs the half-width in the model problem used throughout this paper would be expected to decay to zero as the VT state is stabilized by the added potential ZV_{att} . Why? As Z increases, the VT state's wave function becomes more radially compact while the DC state whose energy is (nearly) degenerate with that of the VT state becomes more radially extended (i.e., of lower kinetic energy). As a result, the coupling matrix element between these two states will decrease. But to what extent does the factor $\sqrt{Z_0 - Z}$ (or low powers of this factor) describe the Z dependence of the half-width (e.g., such as the data shown for N_2^- in Figure 9)? It would be nice to learn more about this issue.

- As another test of one's EM for the data of Figure 5, one could remove one or more of the DC states that undergo avoided crossings with the VT state to see to what extent the EM can predict the correct energy and half-width if there are few or many DC states lying between $E = 0$ and the $Z = 0$ value of the real part of the metastable state's energy. The correct energy and half-width are given in ref 16. Knowing the answer to this question may be important because it might turn out that one needs to have quite a few DC states separating $E = 0$ and the final E of the metastable state to achieve reliable results. On the other hand, it might turn out that one's EM performs best when there is only one DC state present (e.g., one near the final E of the metastable state).
- When developing SM approaches that contain two-branch (or more) functional forms such as the GPAs in eq 10 but with the intent to focus on using E data from only the VT branch, it would be wise to compare the dependence of the results obtained on the energy precision limit (e.g., 10^{-5} eV) and on the locations of the Z_k data points when one uses data from both branches. In other words, is it better to focus on a method that can use two E values for each Z_k data point than to insist on using a one-branch approach? I expect that using data (of precision 10^{-5} eV) from two branches would allow one to select Z_k values farther from the avoided crossing than if one restricts the data to the VT branch alone.

5. CONCLUSIONS

I have attempted to explain how stabilization and extrapolation methods that utilize energy data from conventional electronic structure calculations are used to determine the energies and half-widths of electronically metastable states. In so doing, I focused on the following: (i) the functional forms $E(Z)$ used to relate the energy data E to the parameter Z used to characterize the strength of the variation used in the SM or EM; (ii) the need to limit SM or EM formulas to those whose parameters can be determined by using energy data precise to between 10^{-5} and 10^{-7} eV, which is what can be obtained by using modern electronic structure methods; (iii) weaknesses that arise when using data from only one branch of a stabilization plot with comparisons to results obtained when data from both branches are used; (iv) using data generated from an exactly soluble model problem to test SM and EM approaches. In addition, I offered several suggestions for workers to explore in pursuit of more reliable tools for studying this class of metastable states. For scientists interesting in exploring the use of current-generation stabilization or extrapolation methods, I offer the following guidance: (v) Within the stabilization approach, it is better to use energy data from both branches of an avoided crossing than to use data from only the plateau branch (the latter approach requires data of precision that might be outside the scope of current electronic structure codes); (vi) also within the stabilization method, it is wise to estimate the V parameter and the slope difference $\delta\alpha$ from the stabilization plot and to then use $\delta Z \leq \frac{V}{\epsilon} \frac{V}{\delta\alpha}$ and $\delta Z \leq \left(\frac{V}{\epsilon}\right)^{1/3} \frac{V}{\delta\alpha}$ (with $\epsilon \approx 10^{-5}$ eV) to estimate the range of Z values where data should be collected; of course, this approach is most applicable when the two branches of the stabilization plot vary approximately linearly with Z and where the avoided crossing is clear enough to produce a reasonable estimate of V ; (vii) when forming, for example, an RF function to fit to the $E(Z)$ data, limit the values of E used as input to $\pm 10^{-5}$ eV; (viii) when using the extrapolation method, be careful when using a Coulomb or attenuated Coulomb function as the stabilizing potential because doing so can give rise to intruding Rydberg-like states that can limit one's ability to track $E(Z)$ to small values of Z where the bound state evolves into an unbound state; I understand that these singular potentials are likely to continue to be used because they require little to no modification of current computer codes, but it is important to keep the possibility of Rydberg-like states in mind; (ix) when fitting computed $E(Z)$ data to an RF to use in extrapolating, find some way (e.g., examining least-squares χ^2 values) to determine to what extent the energy values predicted by the RF vary if small variations are made to the parameters appearing in the RF; (x) watch out if major changes in the computed energies and half-widths arise when the polynomial orders appearing in the numerator and denominator of the RF are increased; this suggests that the number of data points and/or the energy precision (again, limit these to $\pm 10^{-5}$ eV) are not adequate to reliably determine these parameters

■ ASSOCIATED CONTENT

SI Supporting Information

The Supporting Information is available free of charge at <https://pubs.acs.org/doi/10.1021/acs.jpca.1c03920>.

Discussion of how overlap and coupling are connected; demonstration of how approaches of refs 20 and 21 can

give the same result; the issue of energy precision within the extrapolation methods (PDF)

■ AUTHOR INFORMATION

Corresponding Author

Jack Simons – Henry Eyring Center for Theoretical Chemistry, Department of Chemistry, University of Utah, Salt Lake City, Utah 84112, United States; orcid.org/0000-0001-8722-184X; Email: jack.simons@utah.edu

Complete contact information is available at: <https://pubs.acs.org/10.1021/acs.jpca.1c03920>

Notes

The author declares no competing financial interest.

■ ACKNOWLEDGMENTS

I thank the University of Utah Chemistry Department and Henry Eyring Center for Theoretical Chemistry for continued support and the three reviewers for much constructive feedback.

■ REFERENCES

- (1) Jordan, K. D.; Voora, V. K.; Simons, J. Negative Electron Affinities from Conventional Electronic Structure Methods. *Theor. Chem. Acc.* **2014**, *133*, 1445.
- (2) Jagau, T.-C.; Bravaya, K. B.; Krylov, A. I. Extending Quantum Chemistry of Bound States to Electronic Resonances. *Annu. Rev. Phys. Chem.* **2017**, *68*, 525–553.
- (3) Moiseyev, N. *Non-Hermitian Quantum Mechanics*; Cambridge University Press: Cambridge, 2011.
- (4) Taylor, H. S. Models, Interpretations, and Calculations Concerning Resonant Electron Scattering Processes in Atoms and Molecules. *Adv. Chem. Phys.* **2007**, *18*, 91–147.
- (5) Hazi, A. U.; Taylor, H. S. Stabilization Method of Calculating Resonance Energies: Model Problem. *Phys. Rev. A: At., Mol., Opt. Phys.* **1970**, *1*, 1109–1120.
- (6) Jordan, K. D. Construction of Potential Energy Curves in Avoided Crossing Situations. *Chem. Phys.* **1975**, *9*, 199–204.
- (7) Chao, J. S.-Y.; Falcetta, M. F.; Jordan, K. D. Application of the Stabilization Method to the N₂-(X²Π_g) and Mg-(12P) Temporary Anion States. *J. Chem. Phys.* **1990**, *93*, 1125–1135.
- (8) Haritan, I.; Moiseyev, N. On the Calculation of Resonances by Analytic Continuation of Eigenvalues from the Stabilization Graph. *J. Chem. Phys.* **2017**, *147*, 014101–9.
- (9) In this paper, I will not discuss any particular such method for obtaining the energies of several electronic states of the same symmetry to retain my focus on the stabilization and extrapolation methods.
- (10) Nestmann, B.; Peyerimhoff, S. D. Calculation of the discrete component of resonance states in negative ions by variation of nuclear charges. *J. Phys. B: At. Mol. Phys.* **1985**, *18*, 615–626.
- (11) Nestmann, B. M.; Peyerimhoff, S. D. CI method for determining the location and width of resonances in electron-molecule collision processes. *J. Phys. B: At. Mol. Phys.* **1985**, *18*, 4309–4319.
- (12) Horáček, J.; Mach, P.; Urban, J. Calculation of S-Matrix Poles by Means of Analytic Continuation in the Coupling Constant: Application to the ²Π_g State of N₂⁻. *Phys. Rev. A: At., Mol., Opt. Phys.* **2010**, *82*, 032713.
- (13) Papp, P.; Matejčík, S.; Mach, P.; Urban, J.; Paidarova, I.; Horáček, J. Analytical Continuation in Coupling Constant Method; Application to the Calculation of Resonance Energies and Widths for Organic Molecules: Glycine, Alanine and Valine and Dimer of Formic Acid. *Chem. Phys.* **2013**, *418*, 8–13.
- (14) Horáček, J.; Paidarová, I.; Čurík, R. Determination of the Resonance Energy and Width of the 2B_{2g} Shape Resonance of Ethylene with the Method of Analytical Continuation in the Coupling Constant. *J. J. Phys. Chem. A* **2014**, *118*, 6536–6541.

- (15) Landau, A.; Haritan, I.; Kaprálová-Žďánská, P. R.; Moiseyev, N. Atomic and Molecular Complex Resonances from Real Eigenvalues Using Standard (Hermitian) Electronic Structure Calculations. *J. Phys. Chem. A* **2016**, *120*, 3098–3108.
- (16) Sommerfeld, T.; Ehara, M. Short-range stabilizing potential for computing energies and lifetimes of temporary anions with extrapolation methods. *J. Chem. Phys.* **2015**, *142*, 034105–9.
- (17) White, A. F.; Head-Gordon, M.; McCurdy, C. W. Stabilizing potentials in bound state analytic continuation methods for electronic resonances in polyatomic molecules. *J. Chem. Phys.* **2017**, *146*, 044112.
- (18) Whitehead, A.; Barrios, R.; Simons, J. Stabilization calculation of the energy and lifetime of metastable SO₄²⁻. *J. Chem. Phys.* **2002**, *116*, 2848–2851.
- (19) Gasperich, K.; Jordan, K. D.; Simons, J. Strategy for Creating Rational Fraction Fits to Stabilization Graph Data on Metastable Electronic States. *Chem. Phys.* **2018**, *515*, 342–349.
- (20) Carlson, B. J.; Falcetta, M. F.; Slimak, S. R.; Jordan, K. D. A Fresh Look at the Role of the Coupling of a Discrete State with a Pseudocontinuum State in the Stabilization Method for Characterizing Metastable States. *J. Phys. Chem. Lett.* **2021**, *12*, 1202–1206.
- (21) Simons, J. Resonance Lifetimes from Stabilization Graphs. *J. Chem. Phys.* **1981**, *75*, 2465–2467.
- (22) Löwdin, P. O. Approximate calculation of lifetimes of resonance states in the continuum from real stabilization graphs. *Int. J. Quantum Chem.* **1985**, *27*, 495–500.
- (23) Thompson, T. C.; Truhlar, D. G. New Method for Estimating Widths of Scattering Resonances From Real Stabilization Graphs. *Chem. Phys. Lett.* **1982**, *92*, 71–75.
- (24) McCurdy, C. W.; McNutt, J. F. On the Possibility of Analytically Continuing Stabilization Graphs to Determine Resonance Positions and Widths Accurately. *Chem. Phys. Lett.* **1983**, *94*, 306–310.
- (25) Isaacson, A. D.; Truhlar, D. G. Single-root, Real-basis-function Method with Correct Branch-point Structure for Complex Resonance Energies. *Chem. Phys. Lett.* **1984**, *110*, 130–134.
- (26) Frey, R. F.; Simons, J. Resonance State Energies and Lifetimes via Analytic Continuation of Stabilization Graphs. *J. Chem. Phys.* **1986**, *84*, 4462–4469.
- (27) Landau, A.; Haritan, I. The Clustering Technique: A Systematic Search for the Resonance Energies Obtained via Padé. *J. Phys. Chem. A* **2019**, *123*, 5091–5105.
- (28) Puiatti, M.; Vera, M. A.; Pierini, A. B. In search of an optimal methodology to calculate the valence electron affinities of temporary anions. *Phys. Chem. Chem. Phys.* **2009**, *11*, 9013–9024.
- (29) Horáček, J.; Paidarova, I.; Čurik, R. On a simple way to calculate electronic resonances for polyatomic molecules. *J. Chem. Phys.* **2015**, *143*, 184102–7.
- (30) Krasnopolsky, V. M.; Kukulin, V. I. Theory of resonance states based on analytical continuation of the coupling constant. *Phys. Lett. A* **1978**, *69*, 251–254.
- (31) Stillinger, F. H. Ground-State Energy of Two-Electron Atoms. *J. Chem. Phys.* **1966**, *45*, 3623–3631.
- (32) Domcke, W. Analytic theory of resonances and bound states near Coulomb thresholds. *J. Phys. B: At. Mol. Phys.* **1983**, *16*, 359–380.
- (33) Schlessinger, L. Use of Analyticity in the Calculation of Nonrelativistic Scattering Amplitudes. *Phys. Rev.* **1968**, *167*, 1411–1423.
- (34) Bárta, T.; Horáček, J. Calculation of resonances by analytical continuation: role of asymptotic behavior of coupling function. *Phys. Scr.* **2020**, *95*, 065401.